
Article:
Comba, Peter, Nunn, George, Scherz, Frederik et al. (1 more author) (2022) Intermediate-spin iron(IV)-oxido species with record reactivity. FARADAY DISCUSSIONS. pp. 232-244. ISSN 1364-5498

https://doi.org/10.1039/d1fd00073j

Intermediate-spin iron(IV)-oxido species with record reactivity

Peter Comba[a,b] and Frederik Scherz*[a]; George Nunn[c] and Paul H. Walton[c]

a) Universität Heidelberg, Anorganisch-Chemisches Institut, INF 270,

D-69120 Heidelberg, Germany

b) Universität Heidelberg, Interdisziplinäres Zentrum für Wissenschaftliches Rechnen (IWR)

c) Department of Chemistry, University of York, Heslington, YORK, UK, YO10 5DD

Correspondence:

E-mail: peter.comba@aci.uni-heidelberg.de

Abstract

The nonheme iron(IV)-oxido complex *trans*-N3-[(L^1)Fe^{IV}=O(Cl)]$^+$, where L^1 is a derivative of the tetradentate bispidine 2,4-di(pyridine-2-yl)-3,7-diazabicyclo[3.3.1]nonane-1-one, has an S = 1 electronic ground state and is the most reactive nonheme iron model system known so far, of a similar order of reactivity as nonheme iron enzymes (C-H abstraction of cyclohexane, –90 °C (propionitrile), $t_{1/2}$ = 3.5 sec). The reaction with cyclohexane selectively leads to chlorocyclohexane, but "cage escape" at the [(L^1)Fe^{III}-OH(Cl)]$^+$ / cyclohexyl radical intermediate lowers the productivity. Ligand field theory is used herein to analyze the d-d transitions of [(L^1)Fe^{IV}=O(X)]$^{n+}$ (X = Cl, Br, MeCN) in comparison with the thoroughly characterized ferryl complex of tetramethylcyclam (TMC=L^2; [(L^2)Fe^{IV}=O(MeCN)]$^{2+}$). The ligand field parameters and d-d transition energies are shown to provide important information on the triplet-quintet gap and its correlation with oxidation reactivity.

Introduction

The functionalization of hydrocarbon substrates with inert C-H bonds is among the more challenging and important reactions in synthetic organic chemistry.[1-3] Nature frequently uses iron based enzymes for these and other metabolically important oxidative transformations, and nonheme iron(IV)-oxido species have been identified as ubiquitous key intermediates in oxidative transformations of unactivated C-H bonds. The last two decades have seen considerable development in this area, involving enzymatic processes, bioinspired models and technical applications, based on structural data, spectroscopy and mechanistic work and involving experimental as well as computational studies.[4-11] Important and still disputed key questions are related to the importance of the driving force (*i.e.* the $Fe^{IV/III}$-oxido redox potential), where accurate and reliable experimental and computational data still are in demand,[12-17] and the relevance of the spin ground state of the Fe^{IV}-oxido oxidant. All enzymes have an $S = 2$ (high-spin) ground state, while many synthetic model systems are $S = 1$, and those with a quintet ground state are not necessarily the most reactive.[18-23] An important aspect is that, based on ligand field theory, the high-spin ground state is favored for trigonal bipyramidal geometries, as generally observed in enzymes, while many model systems have pseudo-tetragonal coordination geometries, such as those discussed in the present communication. DFT (density functional theory) analysis suggests that C-H abstraction by Fe^{IV}-oxido species generally proceeds on the quintet surface with a preference for the σ channel with a linear [Fe-O···H···C-R] transition state and the electron transferred into the d_{z2} orbital,[24-27] and Fe^{IV}=O oxidants with a triplet ground state generally cross the spin surface to react over the lower energy quintet transition state. The underlying concept of two-state-reactivity (TSR) indicates that the spin ground state of Fe^{IV}=O oxidants might be less important than sometimes assumed, as long as the triplet – quintet energy gap is relatively small.[28-31]

We have recently shown that the Fe^{IV}=O species with the tetradentate bispidine ligand L^1 (bispidine = 2,4-di(pyridine-2-yl)-3,7-diazabicyclo[3.3.1]nonane-1-one, see Scheme 1 for ligands discussed in this manuscript) has an $S = 1$ ground state and is the most reactive Fe^{IV}=O oxidant known so far, probably as fast as enzymes[21-23] – note that a direct comparison of reactivities is difficult because published rates generally have been measured under a variety of conditions and

not such that it would be possible to compare them quantitatively (a relevant collection of rate data is given in Table 1). Important attributes related to the reactivity of $S = 1$ $[(L^1)Fe^{IV}=O(Cl)]^+$ are that (i) the spin crossover, *i.e.* the efficiency of TSR and hence the reactivity of a triplet $Fe^{IV}=O$ oxidant, depends on the triplet-quintet gap,[32-34] (ii) for tetragonal systems, this primarily depends on the in-plane ligand field (see Scheme 2 for a simplified visualization of ligand field effects), and (iii) on the basis of the assignment of the generally observed d-d transitions in analogy to thorough spectroscopic analyses of well-characterized tetragonal ferryl complexes,[35, 36] the relative energy of the in-plane ligand field can be determined experimentally and correlated with the quintet-triplet gap and reactivity, and this is the main contribution of the present communication.

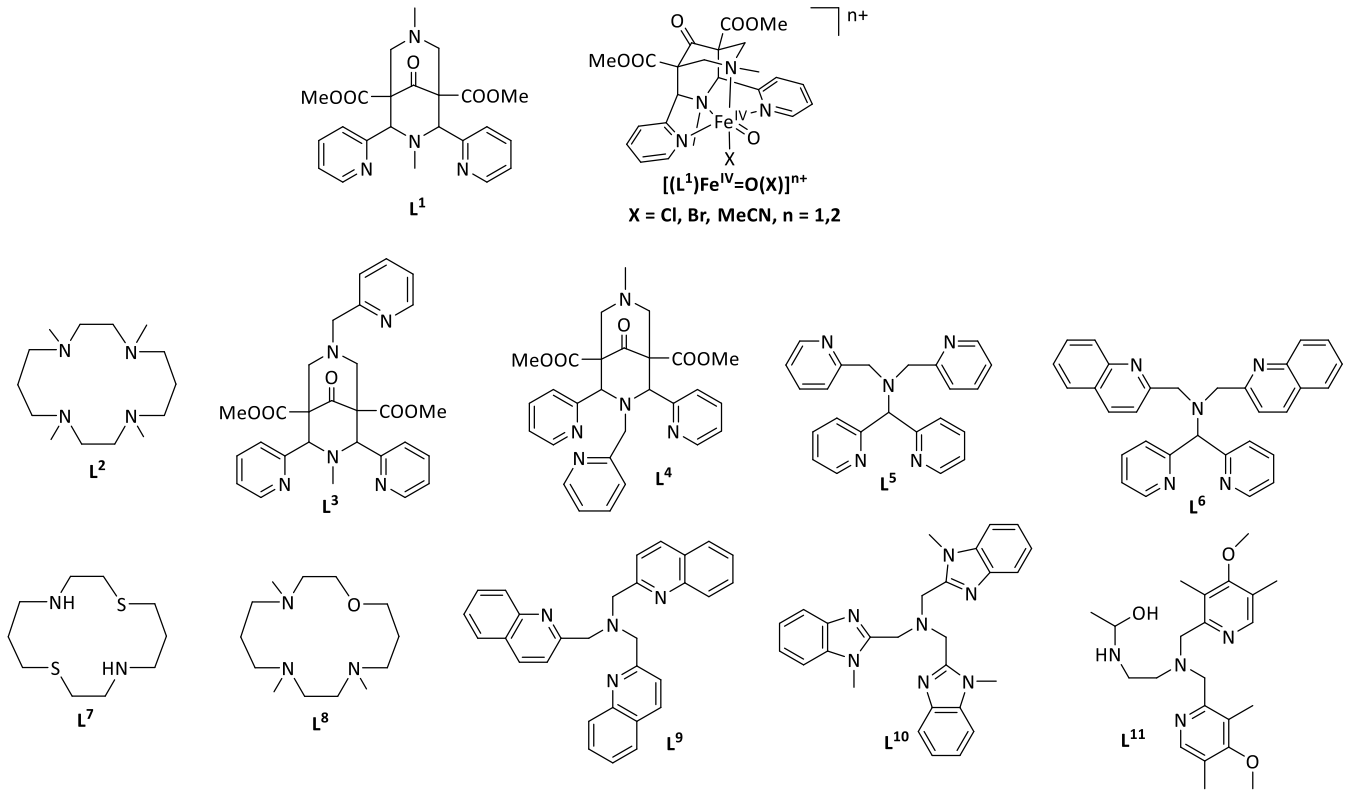

Scheme 1. Ligands discussed in this manuscript and structural drawing of $[(L^1)Fe^{IV}=O(X)]^{n+}$.

Table 1. Selected Pseudo-first-order [s^{-1}] and second order [$M^{-1}s^{-1}$] rates involving mononuclear Fe^{IV}=O species

L / X / spin	dd transition / nm		k / s^{-1}	k / $M^{-1}s^{-1}$	ref
L^1 / MeCN / S = 1	565	786		$1.3\cdot10^{-1}$ a)	15
L^1 / Cl / S = 1	595	850	$2\cdot10^{-1}$ b)	$7.6\cdot10^{2}$ b)	22
L^1 / Br / S = 1	620	900			
L^2 / MeCN / S = 2				$3.7\cdot10^{-1}$ c)	19
L^3 / S = 1	500	730		$4.9\cdot10^{-3}$ a)	15, 37
L^4 / S = 1	500	730		$1.3\cdot10^{-4}$ a)	15, 37
L^5 / S = 1		695		$8.3\cdot10^{-2}$ d)	38
L^6 / S = 1		770		$5.0\cdot10^{-1}$ d)	38
L^7 / MeCN / S = 1	585	848,992		$1.0\cdot10^{-2}$ e)	39
L^8 / MeCN / S = 1	596	815		$3.7\cdot10^{2}$ f)	40
L^9 / MeCN / S = 2				$3.7\cdot10^{-1}$ c)	19
L^9 / Cl / S = 2				$7\cdot10^{-2}$ g)	41
L^9 / Br / S = 2				$5\cdot10^{-2}$ g)	41
L^{10} / - / S = 1	600	770		$2.5\cdot10^{-1}$ h)	42
L^{11} / dinuclear / S = 1				$8.1\cdot10^{-2}$ i)	43
TauD			13 j)		44
MMO				$3\text{-}4\cdot10^{4}$ k)	45, 46

a) cyclohexane, MeCN, -35°C
b) cyclohexane (chlorocyclohexane), EtCN, -90°C
c) cyclohexane (cyclohexanone), MeCN, -40°C
d) bzOH, MeCN, 20°C
e) cyclohexane, CH_2Cl_2, -40°C
f) 1,4-CHD, MeCN, 20°C
g) toluene, MeCN, -40°C
h) cyclohexane, MeCN, -40°C
i) cyclohexane, MeCN, 10°C
j) H_2O, 5°C
k) H_2O, 25°C

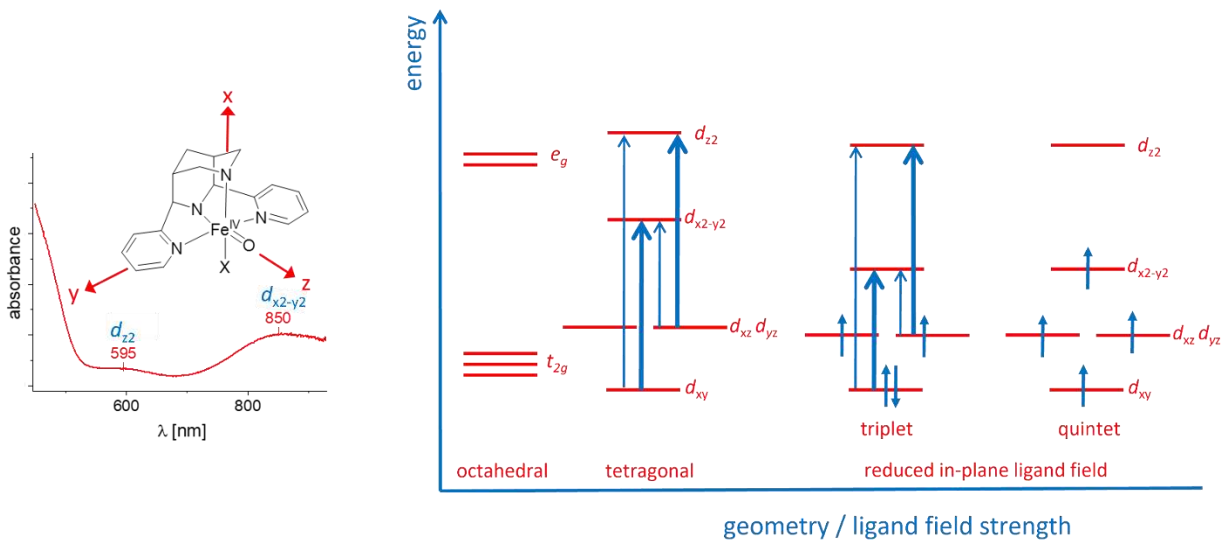

Scheme 2. Structure of of $[(L^1)Fe^{IV}=O(X)]^{n+}$ with the coordinate system used in the ligand field analysis together with the d-d spectrum of the chlorido complex and simplified representation of ligand field effects in pseudo-tetragonal $Fe^{IV}=O$ complexes (bold transitions are those observed in the spectra of $[(L^1)Fe^{IV}=O(Cl)]^+$, all transitions have been assigned for $[(L^2)Fe^{IV}=O(MeCN)]^{n+}$, see below [36]).

While the effect of axial ligands on the reactivities of nonheme $Fe^{IV}=O$ centers has been studied in detail (in heme systems the tuning of reactivities by axial thiolate and selenolate has been shown to be of central importance[34, 47-50]), contrastingly there are only few studies on in-plane ligand field effects with respect to reactivities of nonheme ferryl complexes. [21-23, 38-40, 51, 52] Here we report a thorough analysis of the ligand field properties and possible correlations with the oxidation reactivities of a series $[(L^1)Fe^{IV}=O(X)]^{n+}$ complexes, based on experimental electronic spectroscopic data and ligand field calculations.

Results and Discussion

Experimental spectroscopic and reactivity data

The high reactivity of $[(L^1)Fe^{IV}=O(Cl)]^+$ and derivatives with other co-ligands and to some extent also of ferryl complexes with the pentadentate bispidine ligands L^2 and L^3 bears the problem that $Fe^{IV}=O$ species are difficult to trap and spectroscopically fully characterize – the half-life of $[(L^1)Fe^{IV}=O(Cl)]^+$ at –90°C is only seconds –,[22] and no crystal structures are available of any

bispidine-Fe^{IV}=O complex. Also, Moessbauer and resonance Raman spectra are not yet available from the complexes with the tetradentate bispidine L^1 discussed here, and the electronic spectra are limited to solution UV-vis-NIR measurements obtained a few milliseconds after injecting the oxidant to the iron(II) precursor (see Table 1 and Figure 1). The assignment of the d-d transitions follows those of the fully characterized tetragonal *S* = 1 ferryl complex $[(L^2)Fe^{IV}=O(MeCN)]^{2+}$ based on vis-NIR and MCD spectra supported by experimentally calibrated DFT calculations (see Scheme 2).[36] Reasons for the low in-plane ligand field (low energy of the d_{x2-y2} orbital) in bispidine complexes are that the bispidine cavity is very rigid and relatively large, and that particularly the Fe-N7 bond distance is more flexible and generally longer then the Fe-N3 bond.[53-55] Importantly, the co-ligand X offers an additional simple possibility for tuning the in-plane ligand field.

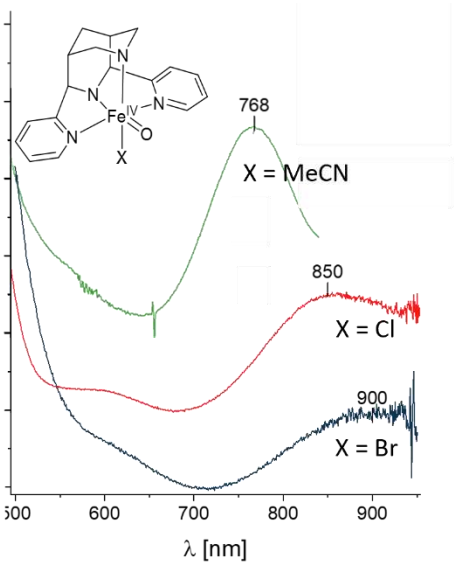

Figure 1. Optical spectra (d-d transitions in the vis-NIR region) of *S* = 1 bispidine-iron(IV)-oxido complexes.

The second problem in terms of data availability is that kinetic studies are hampered by the fact that there are two very fast self-decay processes in addition to reaction with a substrate:[22] the first involves the reaction of the precursor with the product to form an oxido-bridged diiron(III) resting state, *i.e.* an oxo-transfer reaction (OAT) of the ferryl complex. The other is an intramolecular C-H activation (HAT), involving the N7 methyl group and leading to demethylation. From a kinetic analysis of $[(L^1)Fe^{IV}=O(Cl)]^+$ in MeCN at -90°C it follows that even with a 10-fold

excess of iodosylbenzene as oxidant, the pseudo-first-order formation rate of the ferryl oxidant is only just over 5 times larger than HAT with cyclohexane, and the self-decay processes are only 5 (OAT) to 100 (HAT) times slower under these conditions than the reaction with substrate.[22] Preliminary data suggest that the reactivity of the corresponding bromido complex $[(L^1)Fe^{IV}=O(Br)]^+$ for which no full kinetic analysis is available is about one order of magnitude larger than that of the chlorido complex, that of the MeCN complex under similar conditions is around one order of magnitude slower,[21] and this correlates qualitatively with the main dd transition assigned to that to d_{x2-y2} (see Figure 1).

Ligand field analysis

The ligand field computer program, *Kestrel*,[56] (ref. Paul, George) was used for the analysis of the optical spectra of $[(L^1)Fe^{IV}=O(X)]^{n+}$ (X = MeCN, Cl, Br). *Kestrel* uses a configurational interaction method to calculate the ligand field energies of d electron Russell-Saunders states, using the traditional ligand field parameters (Racah B and C, spin-orbit coupling) and angular overlap model (AOM) e-values as inputs. The differences in calculated energies can be fit to experimental transition energies to determine the ligand field parameters. In this case, there are two possible strategies to reduce the complexity of the fitting procedure, *i.e.* to either use pseudo-D_{4h} or pseudo-C_{4h} symmetry of the coordination sphere. The former is less ambiguous and is used here, results of the latter are also discussed in the Supporting Information. With assumed D_{4h} symmetry, one obtains an axial ligand field for the $Fe^{IV}=O$ / Fe^{IV}-NCMe axis of $[(L^2)Fe^{IV}=O(MeCN)]^{2+}$ or the $Fe^{IV}=O$ / Fe^{IV}-N3 axis of $[(L^1)Fe^{IV}=O(X)]^{n+}$ (X = MeCN, Cl, Br), respectively, and an in-plane ligand field for the four tertiary amines of $[(L^2)Fe^{IV}=O(MeCN)]^{2+}$ or N7, the two pyridines and X for $[(L^1)Fe^{IV}=O(X)]^{n+}$ (X = MeCN, Cl, Br), respectively. Note here, therefore, that the calculated e_σ values for the ligating atoms in either axial or equatorial directions represent the *average* e_σ value for each ligating atom in that direction. The π interactions of the tertiary amines as well as the in-plane π interaction of the pyridines are assumed to be negligible.

Initial AOM values were obtained as follows. The thoroughly analyzed spectra (UV-vis-NIR and MCD) of the pseudo-C_{4h} symmetrical $[(L^2)Fe^{IV}=O(MeCN)]^{2+}$,[35, 36] for which also an X-ray structure is available,[57] was modelled with *Kestrel* to yield an initial $e_\sigma(N)$ parameter of 5000 cm^{-1}. The final fitted parameters are presented in Table 2 (see Supporting Information for details of the fitting procedures).

Table 2. AOM parameters [cm^{-1}] for $[(L^1)Fe^{IV}=O(X)]^+$ (X = MeCN, Cl, Br) and $[(L^2)Fe^{IV}=O(MeCN)]^+$.[a]

[cm^{-1}]	L^2 / MeCN[b]	L^1 / MeCN	L^1 / CL	L^1 / Br
e_σ(axial)[c]	10500	10500	10500	10500
e_π(axial)[c]	5750	5450	5500	5400
e_σ(equatorial)[c]	6600	6350	5750	5100
e_π(equatorial)[c]	0	0	0	0

[a] As obtained from an LFT analysis of the UV-vR spectra. Racah B = 400, C/B = 4.

[b] Adapted from an LFT analysis of spectroscopic data of $[(L^2)Fe^{IV}=O(NCCH_3)]^{2+}$.

[c] The complexes are assumed have C_{4v} symmetry, 'axial' refers to the Fe-O axis including the ligand trans to the oxido group (L^2 / MeCN: MeCN; L^1 / X: R_3N3); 'equatorial' denotes the average ligand field strength of the in-plane ligands (L^2 / MeCN: NR_3; L^1 / X: N7, py, py, X).

The final ligand field parameters in Table 2 have been adjusted empirically to the experimental spectra and are general for the d-d spectra of the four ferryl complexes ($[(L^1)Fe^{IV}=O(X)]^+$ (X = MeCN, Cl, Br) and $[(L^2)Fe^{IV}=O(MeCN)]^+$, where the e parameters are as usual adjusted with $1/r^5$, r = Fe-L distance).[58] The electronic parameters are also consistent with preliminary AILFT calculations and, importantly, with parameters used for AOM calculations of various other coordination compounds.[58-60] (Table 3 summarizes the experimentally observed d-d transitions of and $[(L^2)Fe^{IV}=O(MeCN)]^+$ and $[(L^1)Fe^{IV}=O(X)]^+$ (X = MeCN, Cl, Br) together with those computed with the parameters of Table 2. As expected, there is excellent agreement between all observed and computed transitions, where most of the assignments are based on those of the well

characterized TMC ferryl complex $[(L^2)Fe^{IV}=O(MeCN)]^{2+}$ and the results of the ligand field calculations.

An important observation from this analysis is that the position of the major d-d transition at 800 nm, 768 nm, 850 nm, 900 nm, for $[(L^2)Fe^{IV}=O(MeCN)]^{2+}$, $[(L^1)Fe^{IV}=O(MeCN)]^{2+}$, $[(L^1)Fe^{IV}=O(Cl)]^{+}$ and $[(L^1)Fe^{IV}=O(Br)]^{+}$, is not necessarily a direct measure of the $d_{xz/yz}$ to d_{x2-y2} energy gap, due to mixing with the nominal d_{xy} to $d_{xz/yz}$ transition (Figure 2). Using this transition to indicate ligand field strength, and therefore the triplet-quintet energy separation (as per Scheme 2), is therefore an oversimplification. As Figure 2 shows, for lower ligand field strengths the lowest *experimentally* observed transition in the visible spectrum (ie. > 10,000 cm−1) has high d_{xy} to $d_{xz/yz}$ character, the energy of which does not track the variation of the triplet-quintet gap with e_σ ligand field strength (blue line in Figure 2). At higher ligand field strengths the lowest energy *experimentally* observed transition has significantly more $d_{xz/yz}$ to d_{x2-y2} character, which does act as a useful proxy for the triplet-quintet gap. In this regard, it is instructive to re-examine the relatively low energy transition in $[(L^2)Fe^{IV}=O(MeCN)]^{2+}$ at 10600 cm^{-1}, which we assign to a d_{xy} to $d_{xz/yz}$ transition, which—as described above—is not indicative of a low triplet-quintet energy gap. In accord with this assignment, $[(L^2)Fe^{IV}=O(MeCN)]^{2+}$ is a very sluggish oxidant. In the series of bispidine complexes, where only the co-ligand X varies, the low energy transition observed experimentally is a mixed d_{xy} to d_{x2-y2} d_{xy} to $d_{xz/yz}$ transition which follows an energy surface that tracks moderately well the triplet-quintet gap, and the associated increase in reactivity across the series (Table 1).

Table 3. Experimental and AOM-computed[a] electronic transitions of $[(L^1)Fe^{IV}=O(X)]^{+}$ (X = MeCN, Cl, Br) and $[(L^2)Fe^{IV}=O(MeCN)]^{+}$ in cm^{-1}.

ligands	L^2 / MeCN		L^1 / MeCN		L^1 / Cl		L^1 / Br	
	Exp.	AOM	Exp.	AOM	Exp.	AOM	Exp.	AOM
^3H to ^5D gap		9445		8995		7211		5280
$d_{xz},d_{yz} \rightarrow d_{x2-y2}$	12900	12979	13000	13041	11800	11806	11100	11077
$d_{xy} \rightarrow d_{xz},d_{yz}$	10600	10717		10317		9901		8761
$d_{xy} \rightarrow d_{x2-y2}$		20311		17700–22800		15900–21300		14000–19000

$d_{xz}, d_{yz} \rightarrow d_{z2}$	17600	17384	17700	17726	16800	16794	16100	16088
$d_{xy} \rightarrow d_{z2}$	24900	27000–33000		27000–33000		26000–32000		25000–31000

[a)] Parameters from Table 2, Racah B = 400, C/B = 4, no SOC.

The ligand field analysis allowed us to estimate the energy difference between the triplet and quintet states and its variation with ligand field strength (see Table 3). A feature of Kestrel is that the variation of d state energies can be plotted as function of a ligand field variable, akin to a Tanabe-Sugano diagram. Such a variation is shown in Figure 2, where the average equatorial e_σ value is varied. Qualitatively, the energies agree well with the observed trends in reactivity and also with computed quintet – triplet gaps based on various quantum chemical methods, also including coupled cluster calculations.[21] However, the values given in Table 3 need to be considered with caution, and they might be overestimated by a factor of 2 to 5. One possible reason is that these energies depend quite strongly on the Racah parameters, and these are not yet well enough defined – a thorough AILFT study might be able to relieve this problem.

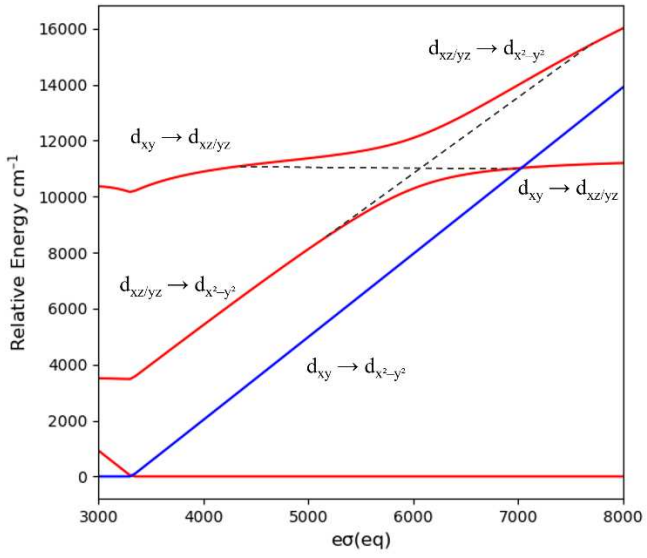

Figure 2. Ligand field calculated energies of d electron states for $[(L^1)Fe^{IV}=O(X)]^+$ where X = exogenous ligand, as a function of average e_σ(equatorial) value. Red lines are triplet d-states, blue line is a quintet d-state.

The ligand field analysis also allowed to obtain the zero-field splitting parameter *D* and, for $[(L^2)Fe^{IV}=O(MeCN)]^+$, it can be compared to experimental data (field Mössbauer: 28 cm^{-1}, HF-EPR: 26.95 cm^{-1} [61] The value computed with the parameters in Table 2 are 27 cm^{-1}, 45 cm^{-1} and 48 cm^{-1} for $[(L^2)Fe^{IV}=O(MeCN)]^{2+}$, $[(L^1)Fe^{IV}=O(MeCN)]^{2+}$, $[(L^1)Fe^{IV}=O(Cl)]^+$ and $[(L^1)Fe^{IV}=O(Br)]^+$, respectively (see Supporting Information). These computed *D* values have to be appreciated as preliminary because, as for the triplet – quintet gaps above, these strongly depend on the parameters used (Racah parameters and spin orbit coupling). However, it appears that within the group of complexes studied here, specifically in the group of the three bispidine complexes, the variation of the electronic parameters should be minimal. The fact that the zero-field splitting increases with decreasing quintet – triplet gap, and that there is a significant increase from the TMC to the bispidine system is expected, and it will be of interest to probe this experimentally. This is of particular importance with respect to an assumed correlation of the triplet – quintet gap with the oxidation reactivity because the spin coupling matrix elements are known to be related to the activation barrier.[21, 32]

Conclusion

$[(L^1)Fe^{IV}=O(Cl)]^+$ as an oxidant for organic substrates, in particular for the difficult to oxidize substrate cyclohexane with less than 10 kcal/mol more activated C-H bonds as the "dream substrate" methane has been studied in detail in terms of oxidation power (driving force), efficiency (activation barrier of the rate determining step) and product selectivity,[15, 22, 23] and has been shown to be the most reactive ferryl oxidant known although it has, in contrast to all enzymes "the wrong spin ground state". The probable reason for this interesting behavior is a very low energy gap between the triplet ground and the quintet excited state, and this has been suspected on the basis of ab-initio quantum chemical calculations.[21] In the current communication we discuss an empirical ligand field analysis involving the AOM analysis of the ligand field spectra of $[(L^1)Fe^{IV}=O(X)]^{n+}$ with X=MeCN, Cl, Br as in-plane ligand with varying donor strength cis to the oxido group. The ligand field analysis indicates that with decreasing ligand field strength (MeCN > Cl > Br) there is a decrease of the triplet – quintet gap concomitant with a shift

of the main dd transition towards lower energy, an increase of the zero-field splitting and an increase of the oxidation reactivity. The present analysis is an excellent qualitative and semi-quantitative basis for a quantitative analysis that most importantly should involve additional spectroscopic techniques and temperature-dependent kinetic analyses, which both are not trivial with an Fe^{IV}=O complex that decays already in absence of external substrates in seconds at -90°C, as well as quantum chemical studies including CASSCF/NEVPT2 optimized wavefunctions and AILFT, which also have limits – not least because the generally DFT-optimized structure might not be in the minimum of the ab-initio wavefunction.

Experimental Section

Details of the Computational Methods

All ligand field calculations were carried out with development version of the Kestrel program, a ligand field program for d-block transition metal compounds.[56](ref. Paul, George) An octahedral preset was chosen, and the axial and equatorial designations were made. The parameters were fitted to the experimental spectra, neglecting some of the π interactions (except for the oxido, the pyridine and halogenide ligands). Transitions were assigned via Tanabe-Sugano plots, connecting the one-electron transitions to the computed many-electron transitions.

Supporting Information

…

Author Information

Corresponding Author

* peter.comba@aci.uni-heidelberg.de

ORCID

Peter Comba: 0000-0002-7796-3532

Acknowledgements

Financial support by the University of Heidelberg and of the German Science Foundation (DFG) is gratefully acknowledged. This study was conducted within the Max Planck School Matter to Life, supported by the BMBF in collaboration with the Max Planck Society. We are grateful for computational resources provided by the bwForCluster JUSTUS, funded by the Ministry of Science, Research and Arts and the Universities of the State of Baden-Württemberg, Germany, within the framework program bwHPC-C5.

Notes

The authors declare no conflict of interest.

References

1. J.-E. Bäckvall, *Modern Oxidation Methods*, Wiley-VCH, 2004.
2. L. Vicens, G. Olivo and M. Costas, *ACS Catal.* , 2020, **10**, 8611-8631.
3. S. Rana, J. P. Biswas, S. Paul, A. Paik and D. Maiti, *Chem. Soc. Rev.*, 2021, **50**, 243-472.
4. C. Krebs, D. Galonici Fujimori, C. T. Walsh and J. M. Bollinger Jr., *Acc. Chem. Res.*, 2007, **40**, 484-492.
5. E. I. Solomon, T. C. Brunold, M. I. Davis, J. N. Kensley, S.-K. Lee, N. Lehnert, F. Neese, A. J. Skulan, Y.-S. Yang and J. Zhou, *Chem. Rev.*, 2000, **100**, 235.
6. M. M. Abu-Omar, A. Loaiza and N. Hontzeas, *Chem. Rev.*, 2005, **105**, 2227-2252.
7. A. R. McDonald and L. Que Jr, *Coord. Chem. Rev.*, 2013, **257(2)**, 414-428.
8. W. Nam, *Acc. Chem. Res.*, 2015, **48**, 2415-2423.
9. W. Nam, Y.-M. Lee and S. Fukuzumi, *Acc. Chem. Res.* , 2014, **47**, 1146-1154.
10. P. Comba, M. Kerscher, M. Krause and H. F. Schöler, *Env. Chem.*, 2015, **12**, 381-395.
11. X. Engelmann, I. Monte-Perez and K. Ray, *Angew. Chem. Int. Ed.* , 2016, **55**, 7632-7649.
12. J. M. Mayer, *Acc. Chem. Res.*, 2011, **44**, 36-46.
13. D. Wang, K. Ray, M. J. Collins, E. R. Farquhar, J. R. Frisch, L. Gomez, T. A. Jackson, M. Kerscher, A. Waleska, P. Comba, M. Costas, E. Münck and L. Que Jr., *Chem. Sci.*, 2013, **4**, 282-291.
14. P. Comba, H. Wadepohl and A. Waleska, *Aust. J. Chem. (Heron 6 Special Issue)*, 2014, **67**, 398-404.
15. P. Comba, S. Fukuzumi, C. Koke, A. M. Löhr and J. Straub, *Angew. Chem. Int. Ed.*, 2016, **55**, 11129-11133.
16. P. Comba, A.-M. Löhr, F. Pfaff and K. Ray, *Isr. J. Chem. (Metal-oxido Special Issue)*, 2020, **60**, 957-962.
17. P. Comba, D. Faltermeier and B. Martin, *Z. Anorg. Allg. Chem. (Special Issue for H. W. Roesky)*, 2020, **646**, 1839-1845.

18. J. England, Y. Guo, K. M. V. Heuvelen, M. A. Cranswick, G. T. Rohde, E. L. Bominaar, E. Münck and L. Que Jr, *J. Am. Chem. Soc.*, 2011, **133**, 11880-11883.
19. A. N. Biswas, M. Puri, K. K. Meier, W. N. Oloo, G. T. Rohde, E. L. Bominaar, E. Münck and L. Que Jr, *J. Am. Chem. Soc.*, 2015, **137**, 2428-2431.
20. C. Kupper, B. Mondal, J. Serrano-Plana, I. Klawitter, F. Neese, M. Costas, S. Ye and F. Meyer, *J. Am. Chem. Soc.* , 2017, **139**, 8939-8949
21. P. Comba, D. Faltermeier, S. Krieg, B. Martin and G. Rajaraman, *Dalton*, 2020, **49**, 2888-2894.
22. M. Abu-Odeh, K. Bleher, N. J. Britto, P. Comba, M. Gast, M. Jaccob, M. Kerscher, S. Krieg and M. Kurth, *Chem. Eur. J.*, 2021, **27**, 11377-11390.
23. K. Bleher, P. Comba, D. Faltermeier, V. Gunasekaran, A. Gupta, M. Kerscher, S. Krieg, B. Martin, H. Wadepohl and S. Yang, *Chem. Eur. J., accepted*, 2021, **27**.
24. S. Ye and F. Neese, *Curr. Opinion Chem. Biol.*, 2009, **12**, 89-98.
25. C. Geng, S. Ye and F. Neese, *Angew. Chem. Int. Ed.*, 2010, **49** 5717-5720.
26. L. Roy, *ChemPlusChem*, 2019, **84**, 893-906
27. D. Mandal, D. Mallick and S. Shaik, *Acc. Chem. Res.*, 2018, **51**, 107-117.
28. S. Shaik, D. Danovich, A. Fiedler, D. Schröder and H. Schwarz, *Helv. Chim. Acta*, 1995, **78**, 1393-1407.
29. D. Schröder, S. Shaik and H. Schwarz, *Acc. Chem. Res.*, 2000, **33**, 139-145.
30. D. Usharani, D. Janardanan, C. Li and S. Shaik, *Acc. Chem. Res.*, 2012, **46**, 471-482.
31. S. Shaik, H. Hirao and D. Kumar, *Acc. Chem. Res.*, 2007, **40**, 532-542.
32. D. Danovich and S. Shaik, *J. Am. Chem .Soc.*, 1997, **119**, 1773-1789.
33. J. Harvey, *Phys. Chem. Chem. Phys.*, 2007, **9**, 331-349.
34. H. Hirao, L. Que Jr., W. Nam and S. Shaik, *Chem. Eur. J.*, 2008, **14**, 1740-1756.
35. A. Decker, J.-U. Rohde, E. J. Klinker, S. D. Wong, L. Que Jr. and E. I. Solomon, *J. Am. Chem. Soc.*, 2007, **129**, 15983-15996.
36. A. Decker, J. U. Rohde, L. Que Jr. and E. I. Solomon, *J. Am. Chem. Soc.*, 2004, **126**, 5378-5379.
37. M. R. Bukowski, P. Comba, A. Lienke, C. Limberg, C. Lopez de Laorden, R. Mas-Balleste, M. Merz and L. Que Jr., *Angew. Chem. Int. Ed.*, 2006, **45**, 3446.
38. G. Mukherjee, C. W. Z. Lee, S. S. Nag, A. Alili, F. G. Cantu Reinhard, D. Kumar, C. V. Sastri and S. P. de Visser, *Dalton Trans.*, 2018, **47**, 14945-14957.
39. I. M. Perez, X. Engelmann, Y.-M. Lee, M. Yoo, E. Kumaran, E. R. Farquhar, E. Bill, J. England, W. Nam, M. Swart and K. Ray, *Angew. Chem. Int. Ed.*, 2017, **56**, 14384-14388.
40. J. Deutscher, P. Gerschel, K. Warm, U. Kuhlmann, S. Mebs, M. Haumann, H. Dau, P. Hildebrandt, U.-P. Apfel and K. Ray Chem. Commun. 2021, 2947-2950, *Chem. Commun.*, 2021, **57**, 2947-2950.
41. M. Puri, A. N. Biswas, R. Fan, Y. Guo and L. Que, *J. Am. Chem. Soc.*, 2016, **138**, 2484-2487.
42. M. S. Seo, N. H. Kim, K.-B. Cho, J. E. So, S. K. Park, M. Clémancey, R. Garcia-Serres, J.-M. Latour, S. Shaik and W. Nam, *Chem. Sci.*, 2011, **2**, 1039-1045.
43. D. Wang, E. R. Farquhar, A. Stubna, E. Münck and L. Que Jr, *J. Am. Chem. Soc.*, 2009, **1**, 145-150.
44. J. C. Price, E. W. Barr, L. M. Hoffart, C. Krebs and J. M. Bollinger Jr., *Biochem.*, 2005, **44**, 8138-8147.
45. A. M. Valentine, S. S. Stahl and S. J. Lippard, *J. Am. Chem. Soc.*, 1999, **121**, 3876-3887.
46. B. J. Brazeau and J. D. Lipscomb, *Biochem.*, 2000, **39**, 13503-13515.
47. T. H. Yosca, J. Rittle, C. M. Krest, E. L. Onderko, A. Silakov, J. C. Calixto, R. K. Behan and M. T. Green, *Science*, 2013, **342**, 825-829.
48. K. Mittra and M. T. Green, *J. Am. Chem. Soc.*, 2019, **141**, 5504-5510.
49. C. V. Sastri, J. Lee, K. Oh, Y. J. Lee, T. A. Jackson, K. Ray, H. Hirao, W. Shin and J. A. Halfen, *PNAS*, 2007, **104 (49)**, 19181-19186.

50. R. Kumar, A. Ansari and G. Rajaraman, *Chem. Eur. J.*, 2018, **24**, 6818-6827.
51. A. Anastasi, P. Comba, J. McGrady, A. Lienke and H. Rohwer, *Inorg. Chem.*, 2007, **46**, 6420-6426.
52. J. Bautz, P. Comba, C. Lopez de Laorden, M. Menzel and G. Rajaraman, *Angew. Chem. Int. Ed.*, 2007, **46**, 8067.
53. P. Comba, M. Kerscher, M. Merz, V. Müller, H. Pritzkow, R. Remenyi, W. Schiek and Y. Xiong, *Chem. Eur. J.*, 2002, **8**, 5750-5760.
54. C. Bleiholder, H. Börzel, P. Comba, R. Ferrari, A. Heydt, M. Kerscher, S. Kuwata, G. Laurenczy, G. A. Lawrance, A. Lienke, B. Martin, M. Merz, B. Nuber and H. Pritzkow, *Inorg. Chem.*, 2005, **44**, 8145-8155.
55. P. Comba, M. Kerscher and W. Schiek, *Prog. Inorg. Chem.*, 2007, **55**, 613-704.
56. P. a. George, *noch einzufügen*.
57. J.-U. Rohde, J.-H. In, M. H. Lim, W. W. Brennessel, M. R. Bukowski, A. Stubna, E. Münck, W. Nam and L. Que Jr., *Science*, 2003, **299**, 1037-1039.
58. P. Comba, *Coord. Chem. Rev.*, 1999, **182**, 343-371.
59. H. Weihe and H. U. Güdel, *J. Am. Chem. Soc.*, 1998, **120**, 2870-2879.
60. M. Atanasov, P. Comba, C. A. Daul and F. Neese, in *Models, Mistery and Magic of Molecules*, eds. J. C. A. Boeyens and J. Ogilvie, Springer, 2008, p. 411.
61. J. Krzystek, J. England, K. Ray, A. Ozarowski, D. Smirnov, L. Que Jr and J. Telser, *Inorg. Chem.*, 2008, **47**, 3483-3485.

TOC

Refs NEU